MMT Observations of the JWST Time Domain Field

Christopher N. A. Willmer[1], R. A. Jansen[2], R. A. Windhorst[2], W. Brisken[3], S. Cohen[2], W. Cotton[3], S. Kattner[4], C. Ly[4], B. Frye[1], A. Koekemoer[5], G. Hasinger[6], V. Jones[2], W.P. Maksym[7], M. J. Rieke[1], I. Smail[8], T. Tyburczy[2], C. White[2]

[1]University of Arizona, [2] Arizona State University, [3] NRAO, [4] MMT Observatory, [5] STScI, [6] ESAC/ESA, Madrid, [7] Harvard-Smithsonian CfA, [8] Durham University

Introduction

Time Domain observations add the critical third dimension used to identify transients. These can range from Near Earth Objects to variable stars, Active Galactic Nuclei and Supernovae. Jansen & Windhorst (2018) proposed using the James Webb Space Telescope (JWST) for time domain observations, which is possible in two small regions within the JWST Continuous Viewing Zones (CVZ) close to the Ecliptic poles. To select the JWST Time Domain Field (TDF), Jansen & Windhorst (2018) examined the distribution of stellar sources and Galactic extinction within both CVZs and identified a region close to the North Ecliptic Pole with few bright stars and low extinction that will be observed as part of R. Windhorst's JWST Guaranteed Time Observations (GTO). To provide a first epoch baseline for the TDF, a multi-observatory effort (Table 1) is being carried out since 2016 to map and classify sources in the region. This poster presents preliminary results coming from the MMT observations.

Table 1: *JWST* **NEP Time-Domain Field multiwavelength community investment**

Telescope	PI	Status	Depth
NuSTAR 3–24 keV	F. Civano	proposed	585 ks; $>$50 cts
Chandra/ACIS-I 0.2–10 keV	W.P. Maksym	in hand; 145 sources	300 ks; $\sim 4.1\times10^{-16}$ cgs
		in progress / proposed	240 ks / 360 ks
XMM-Newton 0.5–2.0 keV	M. Ward / N. Cappelluti	proposed	600 ks; 3×10^{-16} cgs
HST/WFC3+ACS *F275W,F435W,F606W*	R.A. Jansen	in hand; inner $r<5'$ only GO 15278	36 CVZ orbits; $m\sim$ 27.2, 28.2, 29 mag
		proposed	52 CVZ orbits
LBT/LBC U_{sp}*grz*	R.A. Jansen	in hand; wide-field	5 hrs; $m\sim$ 26.5–25.5 mag
Subaru/HSC *giz*,nb816,nb921	G. Hasinger / E. Hu	in hand; wide-field	5 hrs; $m\sim$ 25.5–25.1 mag
GTC/HiPERCAM ugriz	V. Dhillon	proposed; narrow-field	33 hrs; $m\sim$ 28 mag
MMT/MMIRS (img) *YJHK*$_s$	C.N.A. Willmer	in hand	60 hrs; $m\sim$ 22–23
JWST/NIRCam+NIRISS 0.8–5 μm + 1.75–2.23 μm	R.A. Windhorst / H.B. Hammel	*guaranteed time* GTO #1176, #1255	$\sim$49 hrs total; $m<$ 29–28.5 mag
JCMT/SCUBA-2 850μm	I. Smail / M. Im	in progress; $\geq$21 sources	31 hrs; rms $\sim$ 1 mJy
SMA 0.87 mm	G. Fazio	proposed	380 hrs; rms $\sim$ 0.9 mJy
IRAM/Nika2 1.2, 2 mm	S.H. Cohen	in progress	30 hrs; rms $\sim$ 2 mJy
VLA 3(2–4) GHz	R.A. Windhorst/W. Cotton	in hand; $\sim$2500 sources	47 hrs; rms $\sim$ 0.9 μJy
VLBA 4.7 GHz	W. Brisken	in hand; $\sim$200 targets	147 hrs; rms $\sim$ 3 μJy
J-PAS (narrow-band spectroph.)	S. Bonoli / R. Dupke	in progress; ultra-wide field	48 hrs; $m\sim$ 21.5–22.5 mag
MMT/Binospec (mos)	C.N.A. Willmer	in hand; 582 redshifts	18 hrs; $m\sim$ 22.5–24 mag
MMT/MMIRS (mos)	C.N.A. Willmer	proposed	$m<22$, $z>0.4$

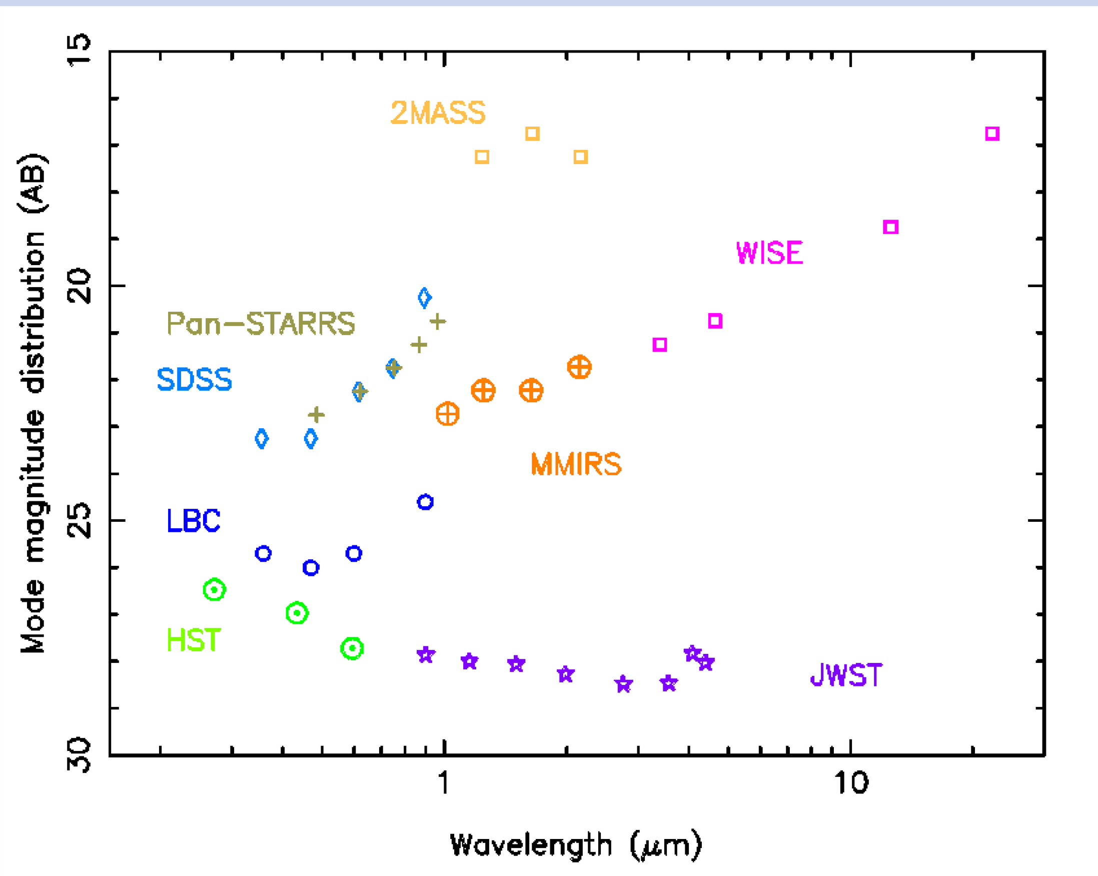

Figure 1. Mode of the magnitude distribution as a function of wavelength for imaging within the TDF footprint. The new observations using HST, the Large Binocular Telescope and MMT provide a first epoch catalogue of sources in the TDF. These observations have already extended in depth, resolution and wavelength range public survey data from SDSS, 2MASS, and Pan-STARRS . The JWST values are estimates for a S/N ~ 5 detection of a point source using the exposure times adopted in R. Windhorst's GTO proposal 1176.

MMT Observations

The MMT has been used to obtain deep near-IR (NIR) imaging and visible spectroscopy of the JWST Time Domain Field (see Table 1). The NIR imaging in Y, J, H, and K bands with MMIRS (McLeod+ 2012) is almost complete, and provides efficient object characterization (Fig. 2). To date, the Visible spectroscopy using Binospec (Fabricant+ 2019) has yielded 552 high confidence new redshifts in this field to r_{AB} ~ 24 mag (Figs. 4 and 5).

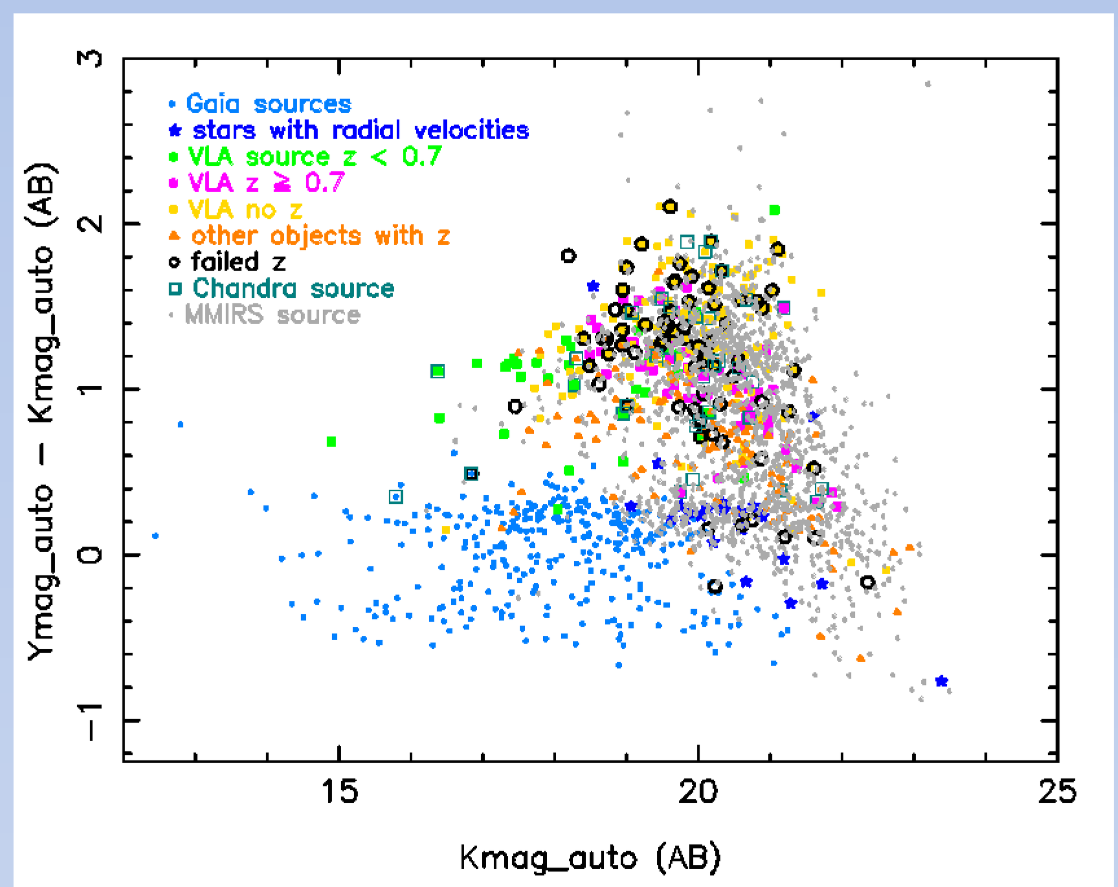

Figure 2. Colour-Magnitude diagram of galaxies in the TDF. The Near Infrared colours are an efficient discriminator between galaxies and stars, particularly those on the main sequence. The key notes several sub-samples of objects. A few galaxies and AGN fall within the locus defined by Gaia sources, while a spectroscopically observed M star falls within the galaxy locus. Most of the objects that did not produce measureable redshifts ("failed z") are concentrated towards red NIR colours, where the majority of galaxies with redshifts > 0.7 are found.

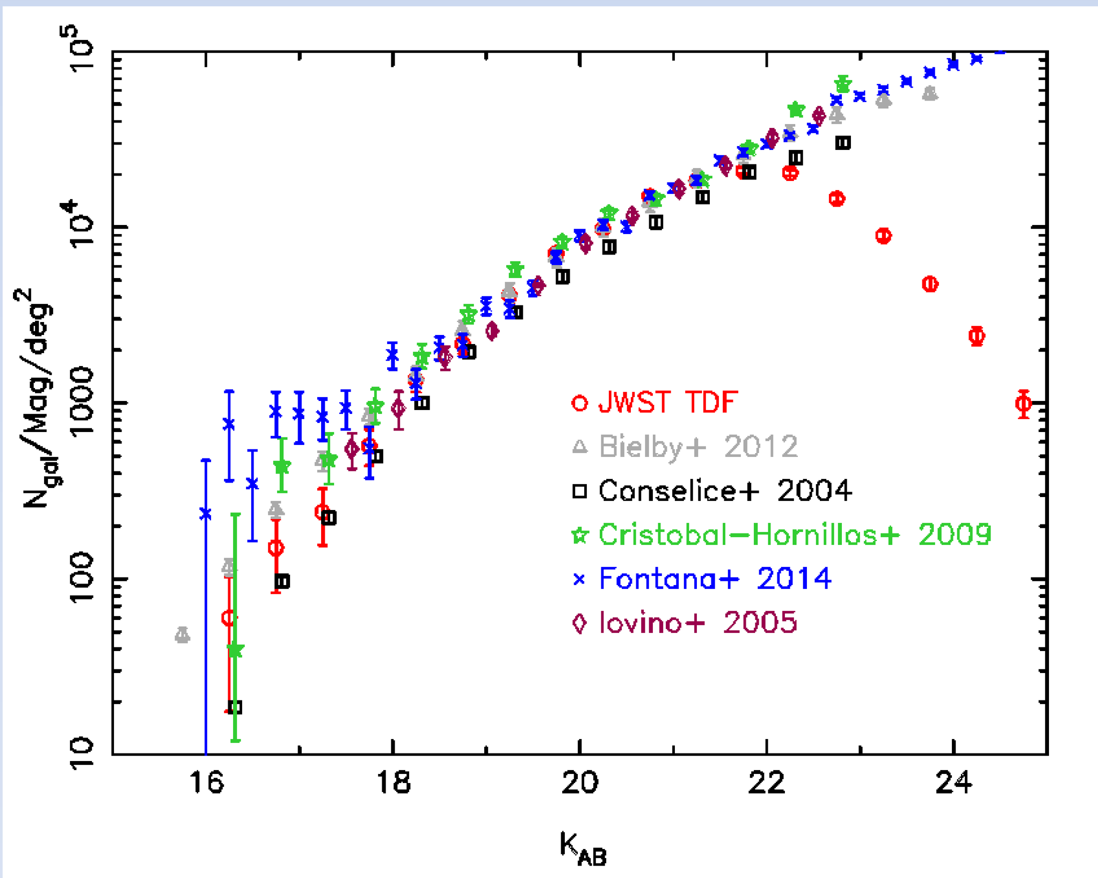

Figure 3. Differential number counts for the TDF area covered by K band (238.9 arcmin^2) after removing contaminating stars using the Gaia classification, the Y-K ≤ 0.4 colour and radial velocities. The counts are not corrected for incompleteness. The number counts suggest that the sample is probably complete to K_{AB}~22. The TDF counts show a behaviour consistent with the published results noted in the key.

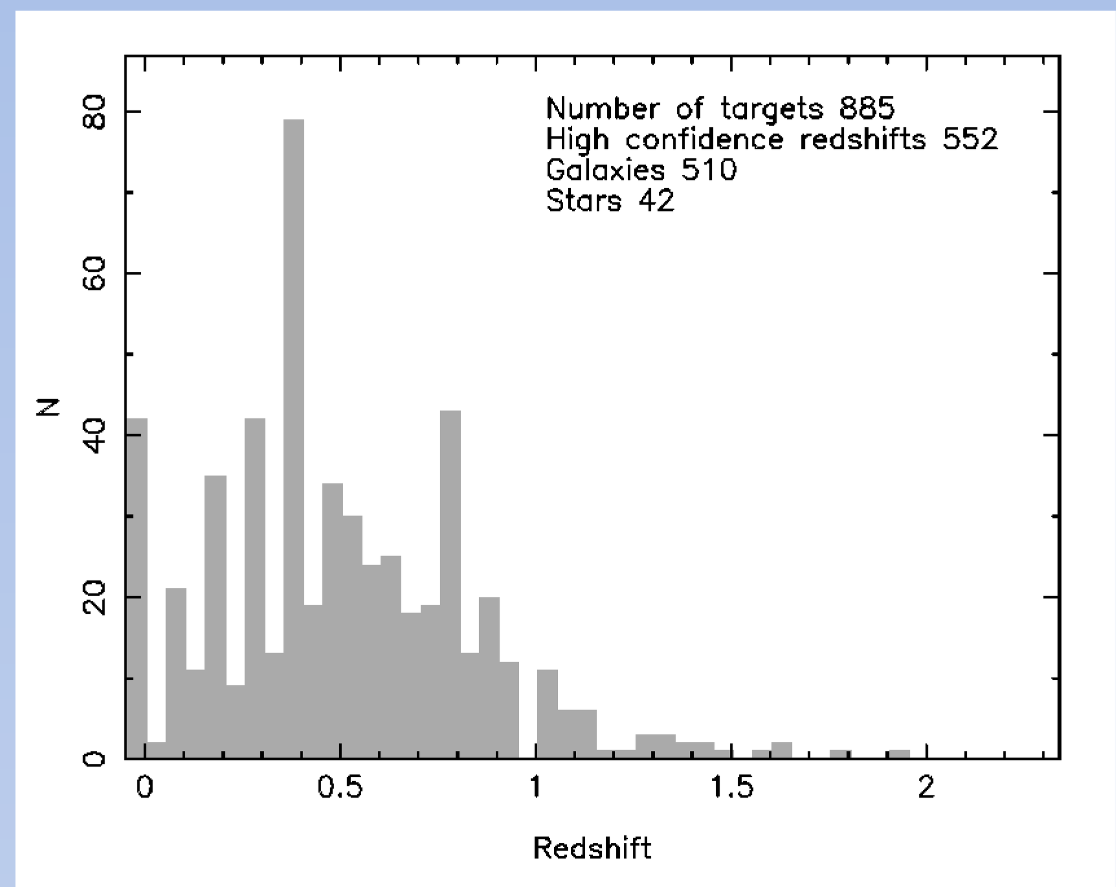

Figure 4. Redshift distribution of galaxies observed in 2018A with MMT/Binospec. Prior to these observations only 4 sources in the TDF footprint had spectroscopic measurements -- 2 stars, a galaxy and a QSO. The redshift survey shows no presence of large density enhancements such as clusters of galaxies to the depth we probe.

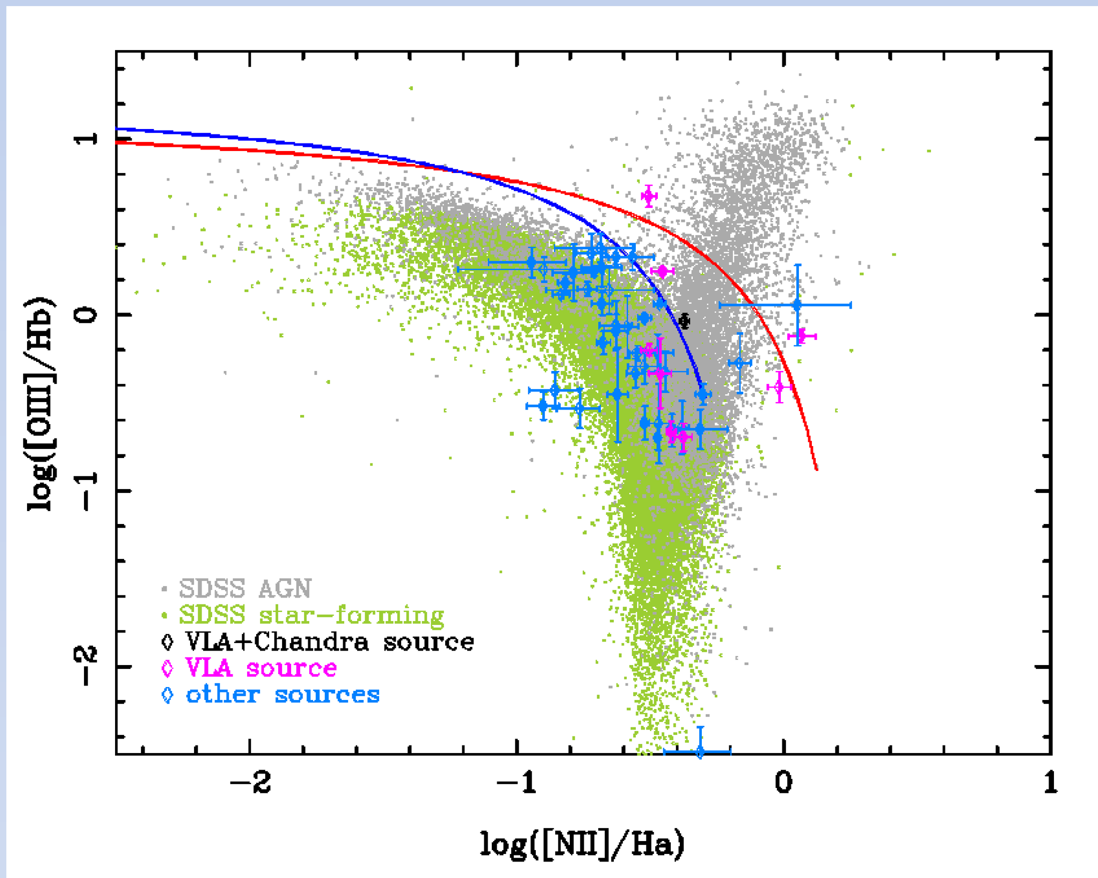

Figure 5. Baldwin, Phillips & Terlevich (1981) diagram for galaxies and AGN in the SDSS DR 7 sample (green and grey dots) and galaxies observed with Binospec (blue, magenta and black points). The curves show the separation between galaxies dominated by star formation (below the curves) and nuclear activity (above the curves) as proposed by Kewley+ 2001 (red) and Kauffmann+ 2004 (dark blue). The sources detected with VLA to ~ 3 μJy are equally distributed among star-forming and powered by Active Galactic Nuclei. No objects with extreme properties (e.g., super metal-poor galaxies) are detected. The AGN already provide a first sample to be monitored for variability.

References

Baldwin, Phillips & Terlevich, 1981, PASP, 93, 5
Bielby+ 2012, A&A, 545, 23
Conselice+ 2008, MNRAS 383, 1366
Cristóbal-Hornillos+ 2003, ApJ, 595, 71
Fabricant+ 2019, PASP in press, ArXiV 1905.03320
Fontana+ 2014, A&A, 570, A11
Iovino+ 2005, A&A, 442, 423
Jansen & Windhorst 2018, PASP, 130, 124001
Kewley+ 2001, ApJ, 556,121
Kauffmann+ 2004, MNRAS, 353, 713
McLeod+ 2012, PASP, 124, 1318